REGULAR ARTICLE

blood advances

An induced pluripotent stem cell model of Fanconi anemia reveals mechanisms of p53-driven progenitor cell differentiation

William Marion,[1] Steffen Boettcher,[2,*] Sonya Ruiz-Torres,[3,*] Edroaldo Lummertz da Rocha,[1] Vanessa Lundin,[1] Vivian Morris,[1] Stephanie Chou,[1] Anna M. Zhao,[1] Caroline Kubaczka,[1] Olivia Aumais,[1] Yosra Zhang,[1] Akiko Shimamura,[1,4,5] Thorsten M. Schlaeger,[1,4] Trista E. North,[1,4] Benjamin L. Ebert,[2,4] Susanne I. Wells,[3] George Q. Daley,[1,4] and R. Grant Rowe[1,4-6]

[1]Stem Cell Program, Boston Children's Hospital, Boston, MA; [2]Division of Hematology, Brigham and Women's Hospital, Boston, MA; [3]Division of Oncology, Cancer and Blood Diseases Institute, Cincinnati Children's Hospital Medical Center, Cincinnati, OH; [4]Harvard Medical School, Boston, MA; and [5]Department of Hematology and [6]Stem Cell Transplantation Program, Dana Farber/Boston Children's Cancer and Blood Disorders Center, Boston, MA

Key Points

- Reversible complementation of FA pathway defects in human IPSCs permits derivation of isogenic mutant and control hematopoietic progenitor cells.
- *FANCA*-deficient cells undergo accelerated erythroid differentiation because of activation of the p53-p21 axis.

Fanconi anemia (FA) is a disorder of DNA repair that manifests as bone marrow (BM) failure. The lack of accurate murine models of FA has refocused efforts toward differentiation of patient-derived induced pluripotent stem cells (IPSCs) to hematopoietic progenitor cells (HPCs). However, an intact FA DNA repair pathway is required for efficient IPSC derivation, hindering these efforts. To overcome this barrier, we used inducible complementation of *FANCA*-deficient IPSCs, which permitted robust maintenance of IPSCs. Modulation of *FANCA* during directed differentiation to HPCs enabled the production of *FANCA*-deficient human HPCs that recapitulated FA genotoxicity and hematopoietic phenotypes relative to isogenic *FANCA*-expressing HPCs. *FANCA*-deficient human HPCs underwent accelerated terminal differentiation driven by activation of p53/p21. We identified growth arrest specific 6 (GAS6) as a novel target of activated p53 in *FANCA*-deficient HPCs and modulate GAS6 signaling to rescue hematopoiesis in *FANCA*-deficient cells. This study validates our strategy to derive a sustainable, highly faithful human model of FA, uncovers a mechanism of HPC exhaustion in FA, and advances toward future cell therapy in FA.

Introduction

Most patients with Fanconi anemia (FA) will develop failure of bone marrow (BM) function, typically occurring in the first decade of life. Curative therapy requires allogeneic hematopoietic stem cell transplantation, a therapy constrained by the availability of human leukocyte antigen matched donors and complications including graft-versus-host disease.[1] Therefore, to benefit patients for whom stem cell transplantation is not an option, investigation has focused on the development of alternative therapies.[2-4] To this end, several model systems have been engineered as platforms for mechanistic investigation of FA hematopoietic progenitor cell (HPC) dysfunction. FA is caused by mutations in at least 22 genes encoding proteins that function in the FA DNA repair pathway.[5] However, knockout of single FA genes in mice typically does not produce HPC failure unless HPCs experience replicative stress, reinforcing the need for human-based systems in which to validate observations made in mouse models.[6-9]

The discovery of human induced pluripotent stem cell (IPSC) technology presented the opportunity for new human FA models.[10] Transduction of terminally differentiated somatic cells such as skin fibroblasts or leukocytes with a defined set of transcription factors confers pluripotency and the capacity for differentiation to tissue derivatives of all 3 embryonic germ layers.[11-13] Because IPSCs share these characteristics with embryonic stem cells, protocols for morphogen directed differentiation of embryonic

Submitted 3 February 2020; accepted 26 August 2020; published online 1 October 2020. DOI 10.1182/bloodadvances.2020001593.

*S.B. and S.R.-T. contributed equally to this study.

RNA sequencing data were uploaded to the Gene Expression Omnibus with accession number GSE123194.

For data sharing requests, e-mail corresponding author, R. Grant Rowe (grant_rowe@dfci.harvard.edu).

The full-text version of this article contains a data supplement.

stem cells to hematopoietic lineages can be applied to patient-derived IPSCs to model blood diseases and investigate new approaches to gene therapy or drug discovery.[11,14,15] Human IPSC-based models have been used to study the BM failure disorders Diamond-Blackfan anemia and Shwachman-Diamond syndrome.[16,17] However, modeling of FA has proven challenging because of the requirement for an intact FA DNA repair pathway for effective induction and maintenance of pluripotency.[18-21] Rescue of FA genetic defects by introduction of a complementing cDNA in FA somatic cells can rescue reprogramming, but permanent repair of FA pathway mutations in IPSCs precludes the downstream derivation of FA-deficient HPCs for disease modeling.[18,19]

Here, we used a system of conditional FA pathway complementation wherein *FANCA*-mutated, patient-derived IPSCs bear an inducible *FANCA* expression cassette.[22] We used these cells in a hematopoietic-directed differentiation system to derive definitive FA HPCs and isogenic control HPCs.[23] *FANCA*-deficient, IPSC-derived HPCs show phenotypes consistent with human FA, including sensitivity to genotoxic stress and diminished clonogenicity in culture. Using this system, we found that activation of the p53/p21 axis in *FANCA*-deficient HPCs hinders cell cycle progression and drives terminal differentiation. We identify growth arrest specific 6 (GAS6) as a target of p53 during differentiation and show that modulation of GAS6 signaling can rescue hematopoiesis in *FANCA*-deficient HPCs. This system overcomes the challenges of studying FA using IPSCs and provides a renewable source of human FA HPCs and isogenic controls for further study of FA pathobiology.

Methods

Cell culture

For embryoid body (EB) formation, IPSCs were plated onto irradiated mouse embryonic fibroblast layers and cultured for 6 to 8 days in the presence of 20% knockout serum replacement (Life Technologies) with 20 ng/mL basic fibroblast growth factor (bFGF; Gibco) and 2 μg/mL doxycycline. Colonies were released by digestion with collagenase IV (Gibco) and cultured under low adherence conditions to form EBs.[23] On day 8, EBs were dissociated, and $CD34^+$ hemogenic endothelium (HE) was affinity purified using anti-human CD34 microbeads (Miltenyi Biotech) and seeded on Matrigel-coated plates.

For endothelial to hematopoietic transition (EHT) culture, cells were cultured in EB medium supplemented with 5 ng/mL bFGF, 15 ng/mL vascular endothelial growth factor, 10 ng/mL interleukin 6 (IL-6), 5 ng/mL IL-11, 25 ng/mL insulin-like growth factor 1, 50 ng/mL stem cell factor, 2 U/mL erythropoietin, 10 ng/mL bone morphogenetic protein 4 (BMP4), 30 ng/mL thrombopoietin, 10 ng/mL Flt3 ligand, and 30 ng/mL IL-3 for 8 days in 5% oxygen (EHT culture). Where indicated, doxycycline was either removed or maintained in culture starting at day 0 of EHT culture. For erythroid differentiation, hematopoietic cells were harvested at day 8 of EHT culture and further cultured in EHT medium. For neutrophil differentiation, EB formation and EHT were performed in the absence of EPO, and nonadherent cells were cultured with 50 ng/mL stem cell factor and 50 ng/mL granulocyte colony-stimulating factor for 4 days, at which time they were analyzed by flow cytometry. Recombinant human GAS6 was used at 800 ng/mL where indicated. For StemDiff culture, IPSCs were cultured with StemDiff reagents per the manufacturer's protocol (StemCell Technologies).

For methylcellulose culture, HPCs were collected at day 5 or 8 of EHT. A total of 1000 to 10 000 viable cells were suspended in 1.5 mL MethoCult SF H4636 (Stem Cell Technologies) supplemented with 50 ng/mL IL-6, 50 ng/mL thrombopoietin, and 50 ng/mL Flt3 ligand. Colonies were enumerated by blinded scoring at day 14. Where indicated, nutlin-3a at a final concentration of 1 μM was added.

Gene editing

IPSCs were transfected using the 4-D nucleofector platform (Lonza) with crRNA/Cas9 ribonucleoprotein complexes (IDT Technologies) and assembled according to the manufacturer's protocol. Transfected cells were enriched for those with biallelic *TP53* inactivation by culture with nutlin-3a at a concentration of 5 μM for 7 days. Frequency of insertions and deletions was measured by deep sequencing of a polymerase chain reaction (PCR) product amplified with primers flanking the crRNA binding site.

Statistics

Analyses were performed using R, Microsoft Excel, and Graphpad Prism. An unpaired Student *t* test was used with a significance cutoff of 0.05 unless otherwise stated. Results are presented as mean ± standard error of mean (SEM) unless otherwise stated.

Flow cytometry

The antibodies used in this study were all against human antigens: anti-CD71 allophycocyanin (APC), anti-GLYA PE-Cy7, anti-CD49d phycoerythrin (PE), anti-CD45 APC, anti-CD45 fluorescein isothiocyanate, anti-Ki67 APC, anti-CD34 PE-Cy7 (all from BD Biosciences), anti-Band 3 fluorescein isothiocyanate (American Research Products), anti-γH2AX (EMD Millipore), and anti-FANCD2 (Novus). Annexin V APC was used (BD Pharmingen).

Cell cycle analysis

Cells were collected in phosphate-buffered saline and fixed with 70% ethanol. FxCycle PI/RNase staining solution (Molecular Probes/Life Technologies) or a combination of 4′,6-diamidino-2-phenylindole (DAPI) counterstain with Ki67 immunostaining was used for flow cytometry analysis.

RNA sequencing

HPCs were collected at day 8 of EHT culture and resuspended in Trizol (Thermo Fisher Scientific) followed by RNA purification and on-column DNAase treatment using the RNeasy Kit (Qiagen). Three biologic replicates for each condition were included. Low input library preparation was performed by the Molecular Biology Core Facility at the Dana-Farber Cancer Institute (Boston, MA). Libraries were sequenced using the Illumina NextSeq 500 Single-End 75 bp platform with expected 400 million read count.

Quantitative PCR

Whole RNA was used to synthesize cDNA using the miScript Reverse Transcription Kit (Qiagen). Primer sequences were as follows—*FANCA* forward: CTTCCGAGAGGTGTTGAAAGA; *FANCA* reverse: GAAGTCCTGCCGTTCAGTATC; *ACTB* forward: GGA TCAGCAAGCAGGAGTATG; *ACTB* reverse: AGAAAGGGTGTA ACGCAACTAA; *CDKN1A* forward: CTGGGGATGTCCGTCAGA AC; *CDKN1A* reverse: CATTAGCGCATCACAGTCGC; *GAS6* forward: ACCTGTGAGGACATCTTGCC; *GAS6* reverse: GGG TCAAAGGTCCGGAAGTC.

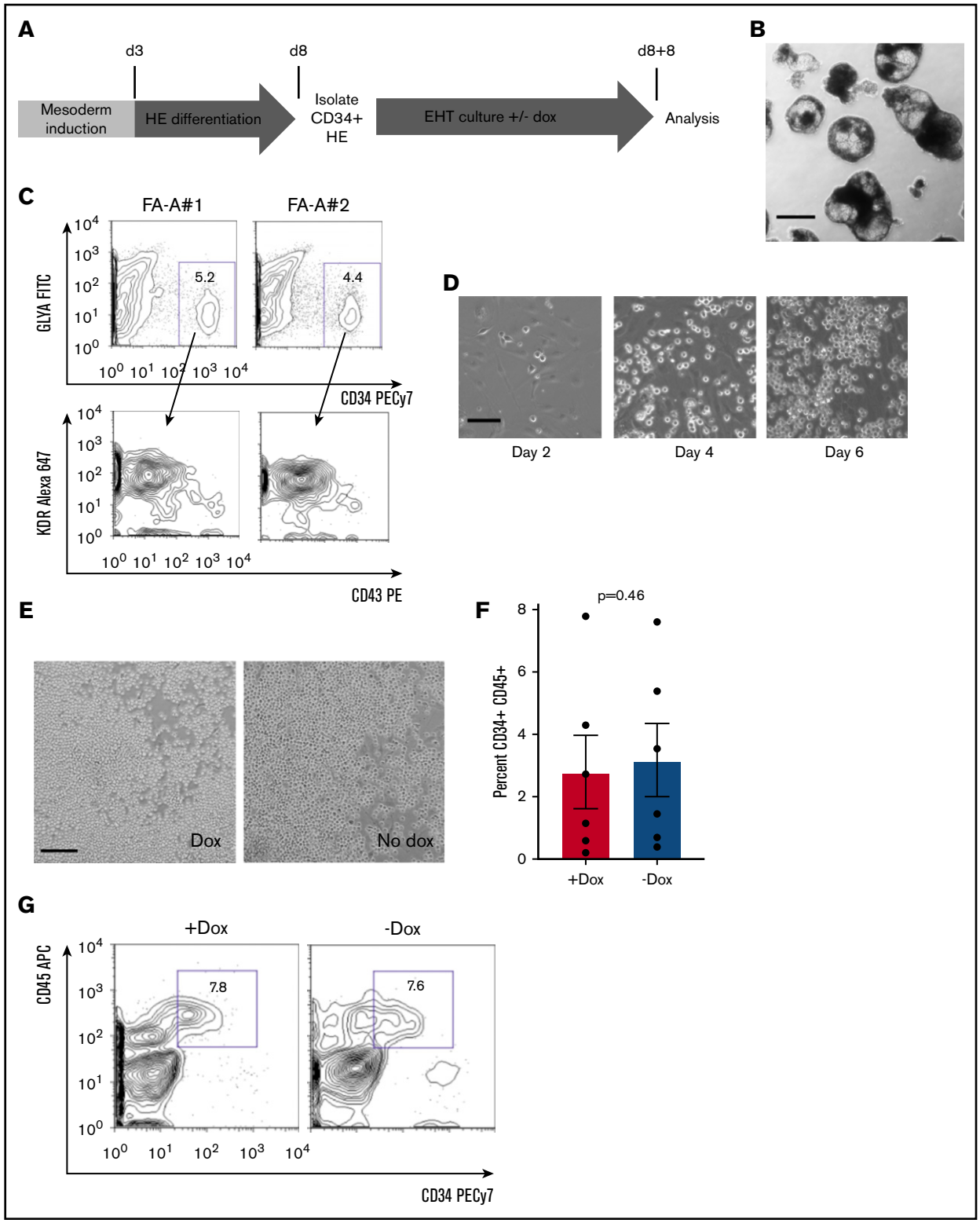

Figure 1. Hematopoietic differentiation of doxycycline inducible human *FANCA* patient IPSCs. (A) Schema for the differentiation of human IPSCs to HPCs adapted from published protocols.[23,27] The first 8-day period involves morphogen-directed specification of hemogenic endothelium within EBs (see "Methods"). This period of culture incorporates 2 phases: BMP-4 and bFGF-mediated mesoderm induction, followed by HE differentiation driven by vascular endothelial growth factor, IL-11, insulin-like growth factor 1, and hematopoietic cytokines. At day 8, EBs were dissociated, and HE was isolated based on $CD34^+$ selection. HE was plated on a 2-dimensional Matrigel substratum for an 8-day EHT culture in the presence of hematopoietic cytokines with or without doxycycline to modulate *FANCA* expression. At the end of the 8-day EHT culture, round floating HPCs were harvested for analysis in assays of clonogenicity and hematopoietic differentiation. (B) Representative image of day 8 EBs before dissociation

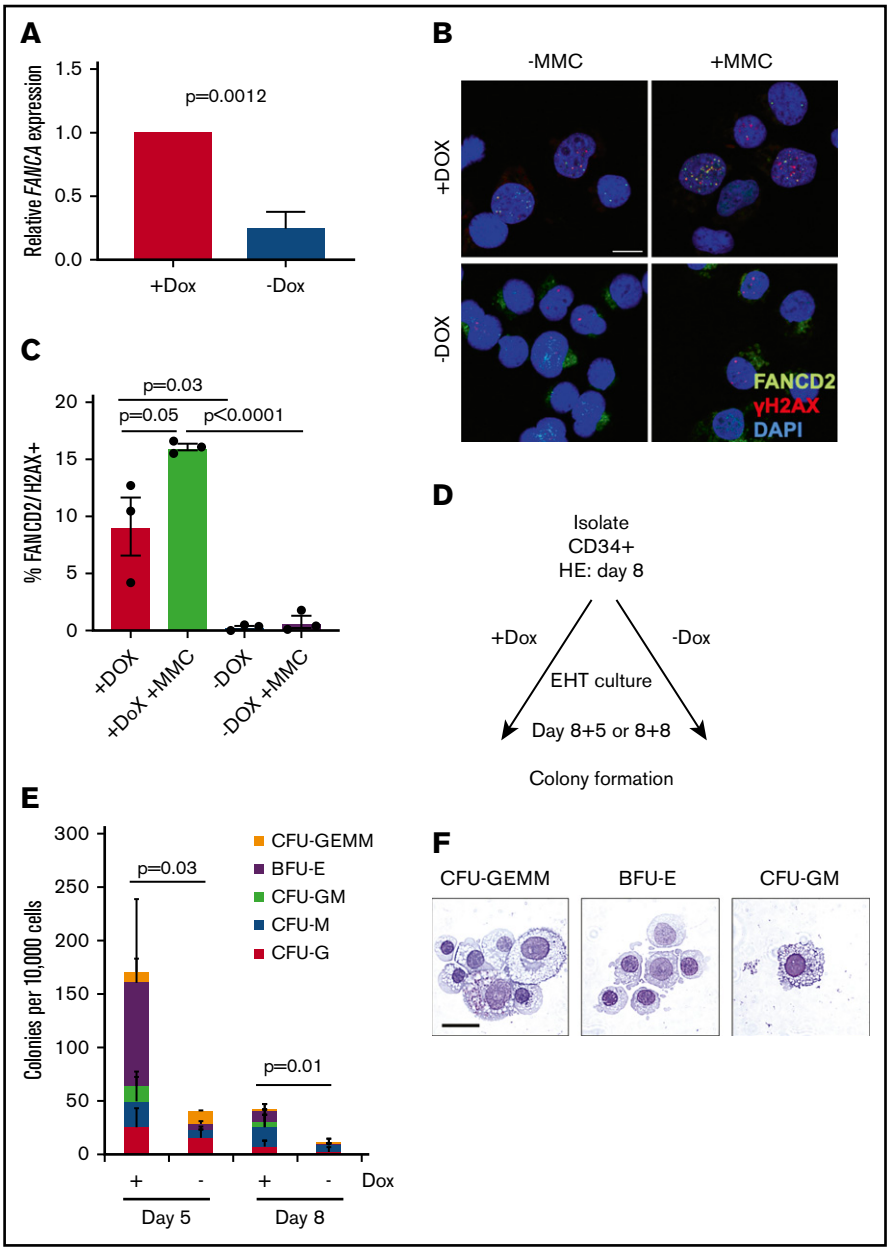

Figure 2. Analysis of *FANCA*-deficient and *FANCA*-expressing IPSC-derived hematopoietic cells. (A) Total RNA was isolated from the nonadherent cells at day 8 EHT, and expression of *FANCA* was analyzed by quantitative PCR (n = 3 biologic replicates; results presented as mean ± SEM, analyzed by a Student *t* test). (B-C) Nonadherent cells were isolated at day 8 of EHT after culture with or without doxycycline and then cultured with mitomycin C (20 ng/mL) for 18 hours, at which time the cells were fixed and immunostained for FANCD2 and γH2AX and visualized by confocal microscopy (scale bar, 10 μm). Results are compiled from 3 separate lines, and the proportion of cells with double-positive foci presented as mean ± SEM, analyzed by a paired Student *t* test. (D-E) A total of 10 000 nonadherent cells collected from day 5 or day 8 EHT cultures were embedded into methylcellulose with hematopoietic growth factors. Doxycycline was either maintained in these assays or withheld consistent with EHT culture conditions. After 14 days, colonies were scored morphologically, and the results were quantified (n = 7 biologic replicates for day 5 and n = 10 biologic replicates day 8 across 3 cell lines; total colony numbers analyzed by a paired Student *t* test, results are presented as mean proportions of each colony type ± standard deviation). (F) Hematopoietic colonies were isolated at day 14 from cultures with doxycycline and spun onto slides when the cells were stained with May-Grünwald-Giemsa and analyzed by light microscopy (scale bar, 10 μm).

Teratoma assay

One million IPSCs were harvested from Matrigel cultures. Cells were resuspended in a 1:1 mixture of DMEM/F12 medium and Matrigel and injected subcutaneously into NOD.Cg-*Prkdc*^{scid} *IL2rg*^{tm1Wjl}/SzJ (NOD/SCID/IL2rγ^{null}; NSG) mice. After 10 to 12 weeks, teratomas were harvested, fixed, embedded, sectioned, and stained for analysis.

Immunofluorescence

For the p53 immunostain, cells were fixed with 4% paraformaldehyde and permeabilized with 0.2% Triton X-100. The DO-7 mouse monoclonal antibody was used (Cell Signaling Technologies) with an Alexa Fluor 594 goat anti-mouse secondary antibody. To costain for FANCD2/γH2AX, cells were fixed with 4% paraformaldehyde and permeabilized with 0.2% Triton X-100 followed by immunostaining

Figure 1. (continued) (scale bar, 200 μm). (C) The entire cellular composition of dissociated day 8 EBs derived from the indicated human IPSC lines was stained with the indicated antibodies and definitive HE (CD34$^+$GLYA$^-$KDR$^+$CD43$^-$) was analyzed by flow cytometry gated on viable singlet cells. (D) Representative images of cultured HE at the indicated time points during EHT culture (scale bar, 50 μm). (E) Representative images of day 8 EHT culture in the presence or absence of doxycycline (scale bar, 100 μm). (F-G) Nonadherent, round cells were harvested at day 8 EHT and analyzed for expression of the indicated surface markers of HPCs by flow cytometry. Percent CD34$^+$ CD45$^+$ HPCs within the nonadherent population was quantified over 6 independent experiments (results presented as mean ± SEM, analyzed by a paired Student *t* test).

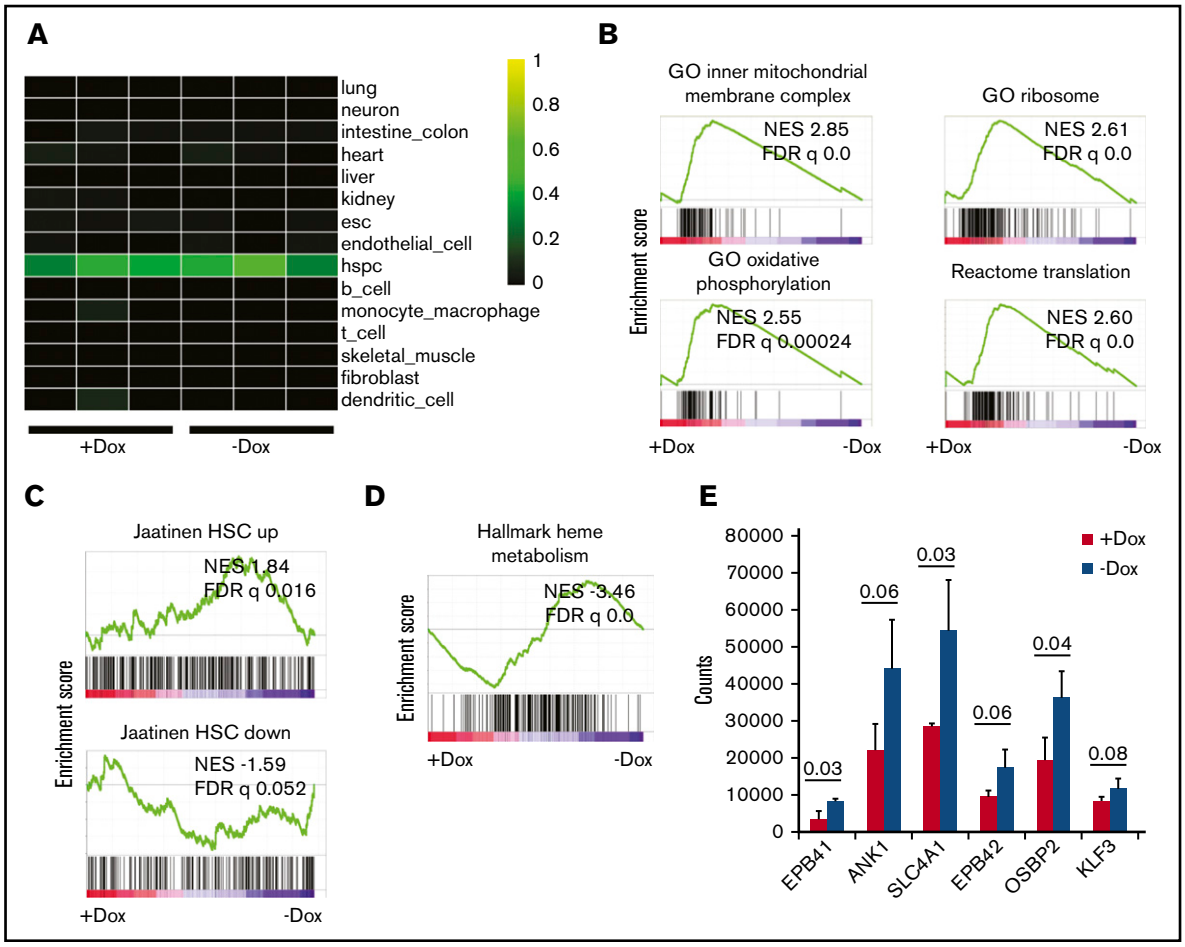

Figure 3. Analysis of gene expression by RNA sequencing. (A) Heatmap showing gene regulatory network enrichment scores as analyzed by CellNet[29] for *FANCA*-expressing (Dox) and *FANCA*-deficient (No dox) hematopoietic cells from day 8 EHT culture. Individual profiles for each of 3 biologic replicates from both cell types are shown. (B) GSEA was used to query the Molecular Signatures Database,[30] and relevant terms enriched in *FANCA*-expressing cells relative to *FANCA*-deficient cells are presented. In all GSEA analyses, a preranked transcript list was used that was compiled from 3 biologic replicates of sequencing for both *FANCA*-expressing and *FANCA*-deficient hematopoietic cells. (C) GSEA was used to query gene sets enriched in human umbilical cord blood HSCs relative to non-HSCs.[33] (D) GSEA was used to query the Molecular Signatures Database, and terms enriched in *FANCA*-deficient cells relative to *FANCA*-expressing cells are presented. (E) Expression of erythroid genes in *FANCA*-expressing vs *FANCA*-deficient hematopoietic cells (analysis with a Student *t* test, n = 3 biologic replicates, results presented as mean ± standard deviation; *P* values are shown).

for FANCD2 (Novus) and γH2AX (EMD Millipore). For quantification of nuclear p53, images were acquired using a 40× lens on a CV7000 CellVoyager Measurement System (version R1.17.06). A script (run on Fiji, V2.0.0-rc-68/1.52g) was used to further process and analyze the images.

Patient cells

FA patient BM aspirates were collected on a human subjects study approved by the Institutional Review Board at Boston Children's Hospital, after informed consent was obtained. This study was performed in accordance with the Declaration of Helsinki. Normal healthy BM mononuclear cells were purchased from AllCells.

Enzyme linked immunosorbent assay

Human GAS6 enzyme linked immunosorbent assay (ELISA) was performed using the Duoset ELISA Kit (R&D Systems).

Results

Directed differentiation of FA IPSCs to HPCs

We used human patient-derived, *FANCA* homozygous mutant IPSC lines that harbor a stably integrated doxycycline-inducible transgene encoding the wild-type *FANCA* open reading frame for inducible and reversible expression.[22] For this study, we used the FA-A#1 and FA-A#2 lines that have previously been characterized as pluripotent[22] and a subclone of FA-A#2 that was verified as pluripotent and euploid in our hands (supplemental Table 1; supplemental Figure 1). For subsequent experiments, unless otherwise indicated, we pooled results from experiments using all 3 of these IPSC lines to limit effects of variability in differentiation potential between lines attributable to background genetic or clonal variation.[24-26]

We adapted previously described protocols of EB-based directed differentiation to generate human HE (Figure 1A).[23,27] For unperturbed

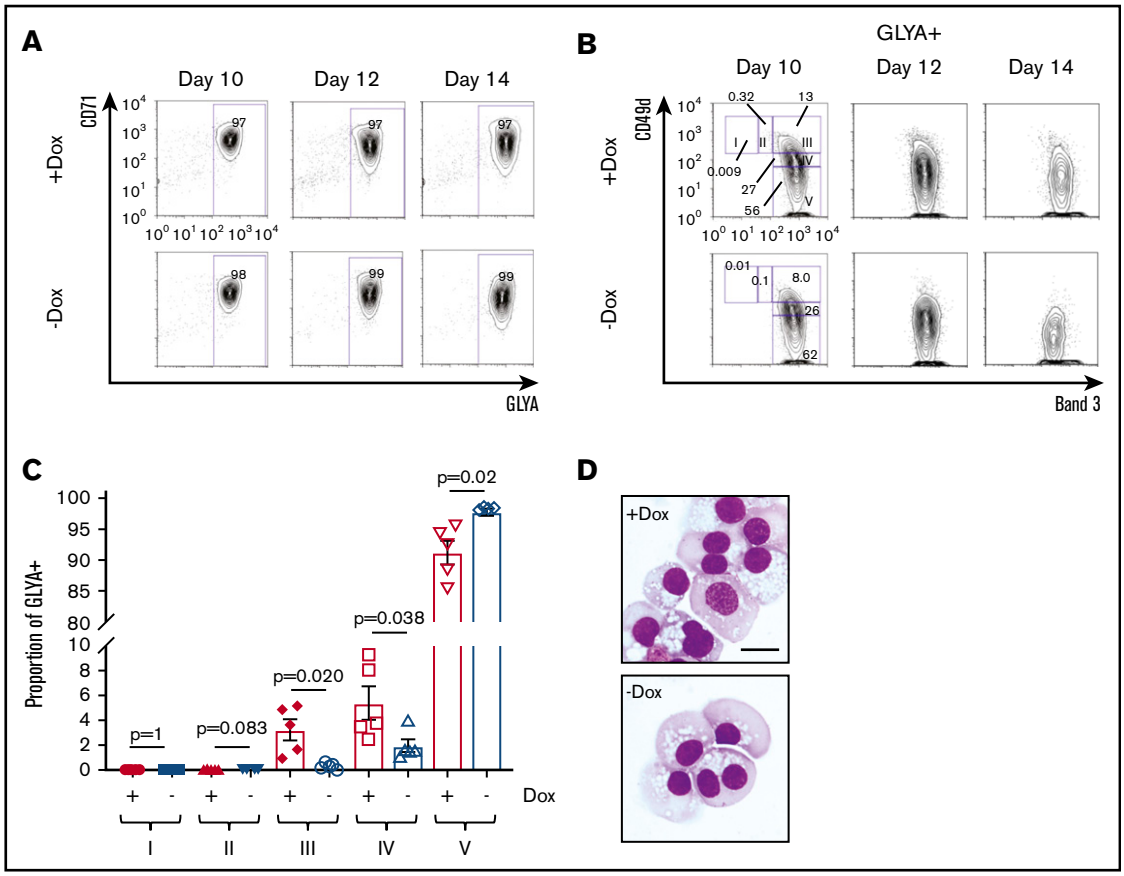

Figure 4. Erythroid differentiation of *FANCA*-expressing or -deficient IPSC-derived hematopoietic cells. (A) Day 8 nonadherent cells from EHT culture were cultured in a cytokine cocktail containing erythropoietin for the indicated periods of time after the initiation of EHT culture, when erythroid differentiation was measured by flow cytometry for CD71 and GLYA expression. (B) Within the GLYA$^+$ gate, cell surface expression of CD49d and Band 3 was measured by flow cytometry. Stages of erythroid differentiation were quantified by gating as described previously.[42] (C) Stages of erythroid differentiation were quantified at day 14, and each stage was compared by a Student *t* test (n = 5 biologic replicates, results presented as mean ± SEM). (D) Representative morphology of day 14 erythroid differentiation culture (scale bar, 10 μm).

directed differentiation and specification of HE, we maintained EBs with doxycycline throughout this 8-day phase of differentiation (Figure 1A). FA IPSCs robustly formed EBs (Figure 1B). We dissociated day 8 EBs and confirmed that we could detect cells expressing a CD34$^+$GLYA$^-$CD43$^-$KDR$^+$ HE immunophenotype (Figure 1C).[23] We isolated HE from dissociated EBs based on surface CD34 and found that adherent HE showed the expected morphology (Figure 1D).

After purification of HE, we initiated EHT culture (Figure 1A). At the initiation of EHT, doxycycline was either removed or maintained for the subsequent 8 days to generate *FANCA*-deficient or *FANCA*-expressing HPCs, respectively (Figure 1A). During EHT, we observed the progressive budding of round, nonadherent human HPCs from the adherent HE layer (Figure 1D), which was not affected by the presence or absence of doxycycline (Figure 1E). Moreover, at the completion of EHT, we detected equivalent proportions of cells expressing the HPC markers CD45 and CD34, further supportive of unimpaired EHT in the absence of doxycycline (Figure 1F-G). As an independent method, we used the StemDiff system, again observing no difference in HPC emergence (Stem Cell Technologies; supplemental Figure 2).

We next examined the status of the FA pathway after EHT. We found that in HPCs generated without doxycycline contained approximately 20% *FANCA* mRNA compared with HPCs generated with doxycycline (Figure 2A). To test the functionality of the FA pathway in response to genotoxic stress, we exposed HPCs to mitomycin C, finding that *FANCA*-deficient cells were unable to localize FANCD2 at sites of DNA damage marked by γH2AX as observed in *FANCA*-expressing cells (Figure 2B-C). These results indicate the absence of functional *FANCA* expression in HPCs emerging in the absence of doxycycline.

Hematopoietic potential of FA HPCs derived from IPSCs

Next, to determine whether our system recapitulates the hallmarks of HPC dysfunction in FA, we examined the hematopoietic capacity of *FANCA*-deficient HPCs.[28] We cultured IPSC-derived HPCs either with or without doxycycline to either maintain or deactivate the inducible *FANCA* transgene, respectively, during assays of hematopoietic function (Figure 2D). In colony formation assays, *FANCA*-deficient HPCs collected at either day 5 or day 8 EHT showed significantly diminished clonogenicity relative to control *FANCA*-expressing cells after 14 days (Figure 2E-F). As expected, colony-forming capacity diminished from day 5 to day 8 because of differentiation of HPCs in culture. We observed similarly impaired

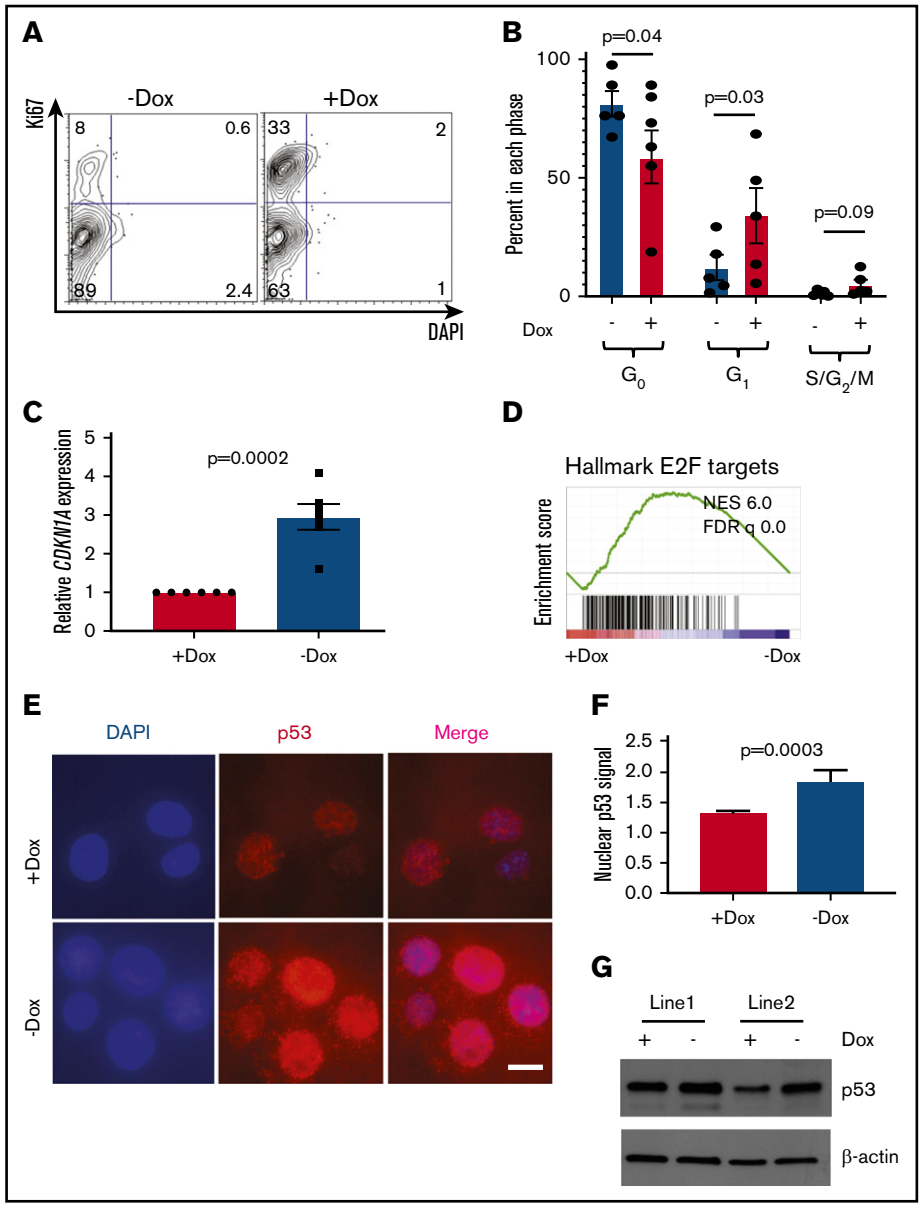

Figure 5. Cell cycle and apoptosis analysis in *FANCA*-expressing and -deficient IPSC-derived hematopoietic cells. (A-B) HPCs were isolated after the completion of EHT culture, at which time they were isolated and stained with DAPI and Ki67 to quantify the cell cycle. The percentage of cells in each phase of the cell cycle was quantified (n = 5 biologic replicates; each phase analyzed by a paired Student *t* test, results are presented as mean ± SEM). (C) Expression level of the *CDKN1A* transcript was measured by quantitative PCR and expression normalized to β-actin mRNA. Expression was compared by Student *t* test with 6 biologic replicates. (D) GSEA analysis of RNA sequencing data. (E-F) Subcellular localization of p53 was analyzed by immunofluorescence staining and nuclear fluorescence signal quantified normalized to DAPI signal (scale bar, 10 μm; results aggregated from 3 biologic replicates, compared by a Student *t* test, results presented as mean ± SEM; n = 240 Dox cells and 111 No dox cells quantified). (G) p53 protein was measured in day 8 EHT HPCs from 2 independent cell lines under the indicated conditions.

clonogenicity of *FANCA*-deficient HPCs derived independently via the StemDiff system and in primary mononuclear cells isolated from FA patients compared with normal healthy control donors (supplemental Figure 2). These results indicate that *FANCA* deficiency in HPCs derived from IPSCs impairs hematopoietic colony formation, recapitulating a known phenotype of HPCs from the BM of human FA patients.[28]

Transcriptional profile of *FANCA*-deficient HPCs

Next, we performed RNA sequencing to evaluate the effect of FANCA deficiency on the transcriptional profile of human IPSC-derived HPCs. Using CellNet, a cell state prediction algorithm,[29] we found that all specimens included in this analysis classified as HPCs without residual signatures of endothelial cells, consistent with unimpaired EHT (Figure 3A). We found 422 transcripts differentially expressed between *FANCA*-expressing and *FANCA*-deficient IPSC-derived HPCs at a significance cutoff of 0.05. We used the Molecular Signatures Database to probe signatures modulated by *FANCA*.[30] Using gene set enrichment analysis (GSEA), we observed enrichment of terms related to mitochondrial respiration in *FANCA*-expressing cells, consistent with a reported role of the FA pathway in regulation of mitochondrial function (Figure 3B).[31,32] Furthermore, we observed signatures consistent with active oxidative phosphorylation, ribosome biogenesis, and translation (Figure 3B; supplemental Figure 3). We found that *FANCA*-expressing HPCs more strongly maintained a normal human HPC signature relative to *FANCA*-deficient HPCs[30,33](Figure 3C). In *FANCA*-expressing cells, we also observed enrichment of signatures related to regulation of the G2/M checkpoint and DNA repair, consistent with the known biology of FA (supplemental Figure 3).[34,35] Moreover, we found signatures associated with the acute inflammatory response including IL-1 and interferon-β production enriched and Toll-like receptors in *FANCA*-deficient cells as has been described previously in mice[36,37] (supplemental Figure 4). We did not observe signatures suggestive

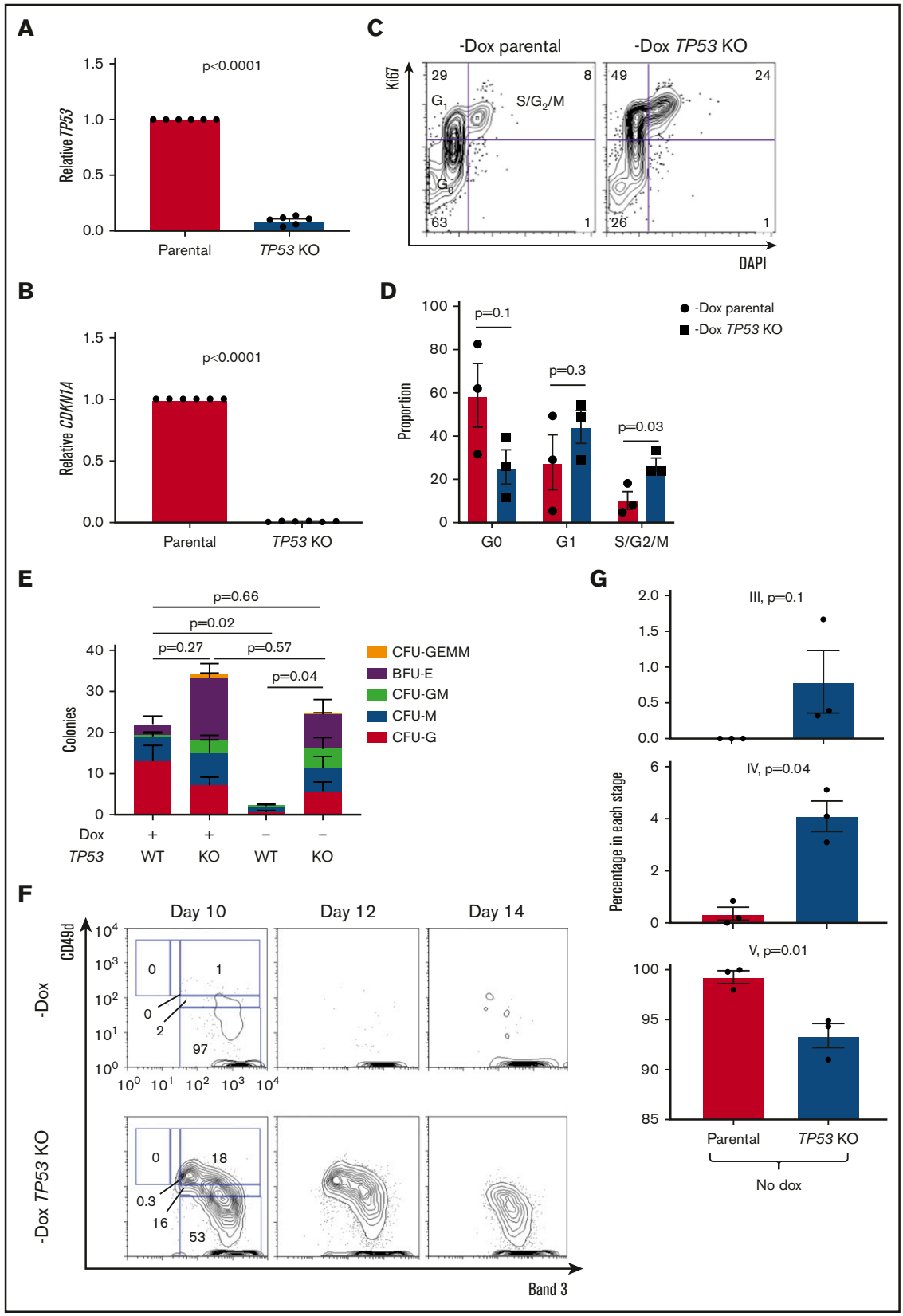

Figure 6. Disabling p53 rescues clonogenesis and slows differentiation in *FANCA*-deficient cells. (A-B) The indicated human IPSC lines were exposed to 1-Gy ionizing radiation, and expression of *TP53* and *CDKN1A* was analyzed 4 hours later by quantitative PCR. Results are aggregated from 2 independent experiments and analyzed by a Student *t* test. (C-D) *FANCA*-deficient HPCs generated in the absence of doxycycline with or without *TP53* disruption were stained for Ki67 and DAPI to analyze

of perturbed transforming growth factor-β signaling in *FANCA*-deficient cells and observed partial overlap with transcripts altered in *Fancd2*$^{-/-}$ mouse hematopoietic stem and progenitor cells vs wild type (supplemental Figure 4).[2,38,39] Interestingly, we found enrichment for transcripts associated with heme metabolism and terminal erythropoiesis in *FANCA*-deficient HPCs, suggestive of an erythroid committed state in these cells (Figure 3D-E). Together, these findings show that our *FANCA*-deficient HPCs bear transcriptional signatures consistent with perturbation of HPC state, recapitulation of known transcriptional signatures associated with FA, as well as a novel signature related to terminal erythropoiesis.

Accelerated terminal differentiation of *FANCA*-deficient HPCs

On further investigation of the pro-erythroid signature observed in *FANCA*-deficient HPCs, we found that these cells expressed higher levels of the downstream erythropoietin signaling components *JAK2* and *STAT5B*, as well as the erythropoietin targets *BCL2L1* and *SOCS3* (supplemental Figure 3).[40] Therefore, we next examined erythropoietin-dependent differentiation.[17,41] Within the GLYA^{+} fraction containing committed erythroid cells, stepwise erythroid differentiation can be examined including proerythroblasts (region I; CD49d^{+}Band 3^{-}), early basophilic erythroblasts (II; CD49d^{+}Band 3^{-low}), late basophilic erythroblasts (III; CD49d^{+} Band 3^{+}), polychromatophilic erythroblasts (IV; CD49d^{-low} Band 3^{+}), and orthochromatophilic erythroblasts (V; CD49d^{-}Band 3^{+}; supplemental Figure 5).[42] Although both *FANCA*-expressing and -deficient cells showed efficient early erythroid commitment with erythroid-induced acquisition of CD71 and GLYA expression (Figure 4A), we found that *FANCA*-deficient HPCs showed accelerated terminal erythroid differentiation (Figure 4B-D). To determine whether this phenotype was specific to erythroid cells, we also tested granulocyte colony-stimulating factor–driven myeloid differentiation, observing an effect suggestive of acceleration in *FANCA* deficient cells (supplemental Figure 6). Together, these findings show that *FANCA* deficiency predisposes HPCs to terminal differentiation.

Impaired cell cycling promotes differentiation of *FANCA*-deficient HPCs

Given the known role of the FA pathway in regulation of the cell cycle and the importance of cycling in differentiation,[35,43,44] we next examined the cell cycle. *FANCA*-deficient HPCs showed a significantly reduced proportion of cells in G_1-phase and a trend toward fewer cells in S/G_2/M-phases consistent with less proliferation (Figure 5A-B). We also observed higher expression of the *CDKN1A* transcript encoding the G_1/S phase checkpoint regulator p21 in *FANCA*-deficient cells (Figure 5C). Consistent with this finding, we observed increased nuclear localization of p53 protein, increased p53 protein levels, and loss of an E2F transcriptional signature in *FANCA*-deficient cells (Figure 5D-G). Increased p53 pathway activation was associated with slightly increased apoptosis in *FANCA*-deficient cells (supplemental Figure 8).

We next examined the connection between *FANCA*, p53, and differentiation. Erythroid differentiation is triggered by GATA1-dependent activation of p21-driven cell cycle arrest rather than apoptosis.[43-45] We found that cell cycling diminishes with progression through erythroid differentiation (supplemental Figure 5). We therefore hypothesized that the enhanced p53/p21 activity in *FANCA*-deficient HPCs augments physiologic expression of p21 to drive erythroid differentiation. To test this, we treated *FANCA*-expressing cells with nutlin-3a, an inhibitor of MDM2-driven p53 degradation. Nutlin-3a induced p21 mRNA expression, impaired colony formation, and accelerated erythroid differentiation in *FANCA*-expressing HPCs (supplemental Figure 7). Thus, activation of p53 is sufficient to augment erythropoietin-induced erythroid differentiation at the expense of clonogenicity.

To further verify this model, we used gene editing to ablate the *TP53* gene in IPSCs followed by treatment of IPSCs with nutlin-3a to increase inserted/deleted allele frequency (supplemental Figure 8). Edited cells were deficient in *TP53* transcripts and could not recruit *CDKN1A* in response to irradiation as expected based on disruption of the *TP53* locus (Figure 6A-B). *FANCA*-deficient, p53-disrupted HPCs showed increased cycling relative to unedited *FANCA*-deficient HPCs (Figure 6C-D). p53 deficiency rescued the impaired clonogenicity of *FANCA*-deficient HPCs (Figure 6E). Moreover, p53 deficiency in *FANCA*-deficient cells slowed progression of erythroid differentiation (Figure 6F-G), establishing p53 as an effector of aberrant HPC differentiation in FA.

GAS6 is a p53 target modulating HPC function

To further investigate the role of p53 in regulating HPC function, we used K562 erythroleukemia cells either deficient for p53 or where the endogenous *TP53* locus was repaired using genome editing.[46] We exposed these cells to hemin to induce erythroid differentiation.[47] We then performed chromatin immunoprecipitation with sequencing for p53, finding that p53 bound the *GAS6* locus (Figure 7A). GAS6 is a known regulator of erythropoiesis.[48] We found that *GAS6* expression was increased in *FANCA*-deficient HPCs relative to controls at the RNA and protein levels (Figure 7B-C). Nutlin-3a increased GAS6 expression, consistent with *GAS6* as a p53 target gene (Figure 7D). We initially hypothesized that p53-driven GAS6 synthesis would negatively regulate HPC function by signaling through its TYRO, AXL, and MER (TAM) receptors. We therefore inhibited TAM signaling in *FANCA*-deficient HPC by using the TAM receptor inhibitor BMS-777607 and activated TAM receptors in *FANCA*-expressing HPCs by exposing them to exogenous GAS6. We found that inhibition of TAM receptors did not rescue clonogenesis in *FANCA*-deficient cells, whereas exogenous GAS6 modestly increased HPC function in *FANCA*-expressing cells (Figure 7E).

Figure 6. (continued) cell cycle status. Results are aggregated from 3 parental IPSC lines and compiled over 2 independent experiments and analyzed by a Student *t* test. (E) The indicated HPCs isolated at day 8 of EHT were plated in methylcellulose in the presence of hematopoietic cytokines (10 000 cells/assay), and 14 days later colonies were scored (n = 4 biologic replicates over 3 independent experiments, and total colony numbers were compared by a Student *t* test, results are presented as mean ± SEM for each aggregated colony type). (F-G) The indicated cell lines were cultured under pro-erythroid differentiation conditions and analyzed by flow cytometry at the indicated time points. CD49d/Band 3 plots are from the GLYA^{+} population of the differentiating culture. Results are aggregated over 3 independent experiments and compared by a Student *t* test.

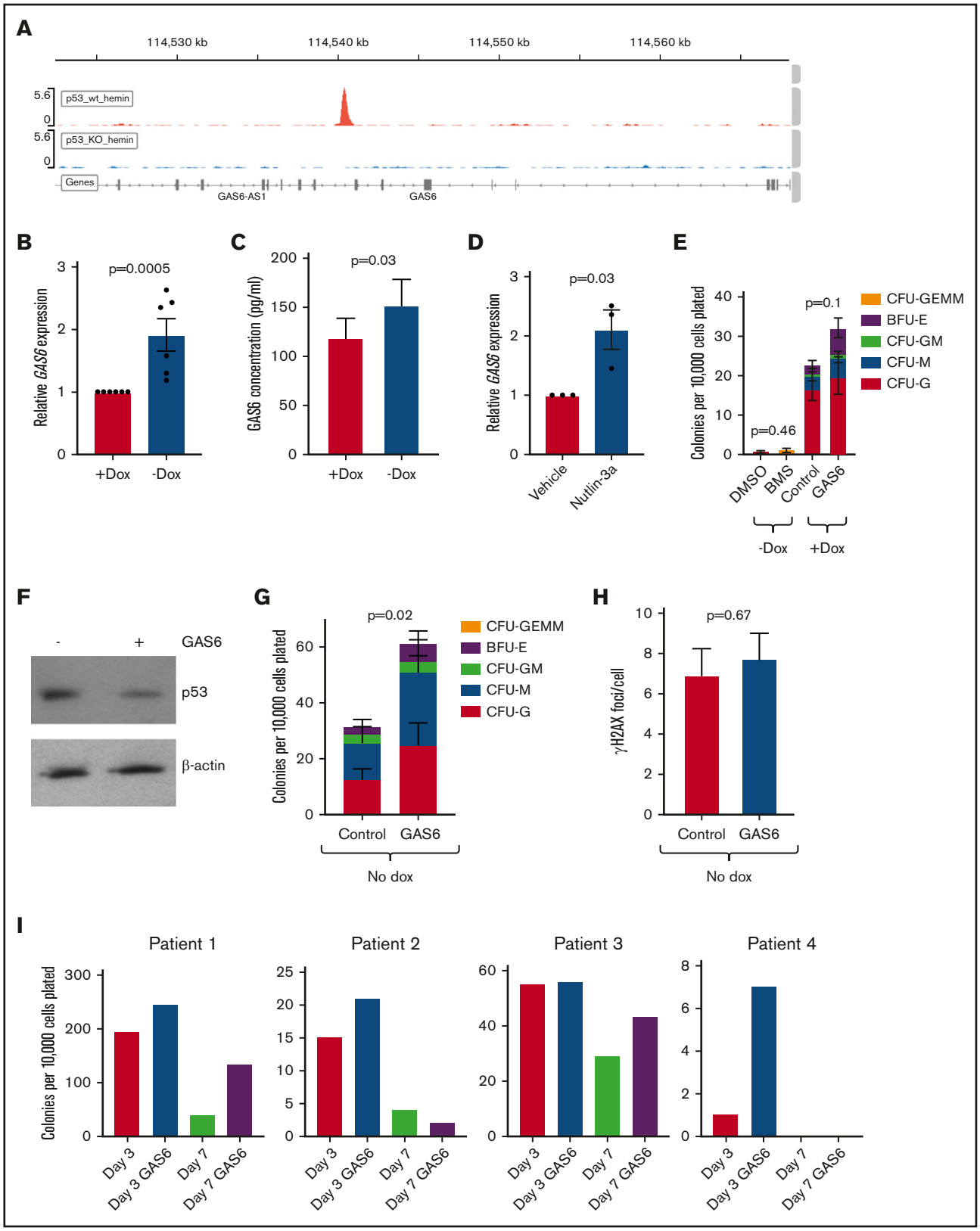

Figure 7. GAS6 is a p53 target in HPCs. (A) p53 wild-type (wt) or knockout (KO) K562 cells were treated with hemin to induce erythroid differentiation for 4 days, at which time chromatin immunoprecipitation for p53 was performed, with peaks at the human *GAS6* locus shown. (B) *FANCA*-expressing or deficient HPCs generated by EHT in the presence of absence of doxycycline, respectively, were collected, and expression of *GAS6* was analyzed by quantitative PCR (n = 6 biologic replicates results). (C) Conditioned culture supernatant of day 8 EHT cells was used for ELISA measurement of GAS6 protein (n = 13 biologic replicates compiled over 2 independent

Given that GAS6 is a prosurvival growth factor, we next hypothesized that p53-induced GAS6 induction acts as a feedback mechanism that could be potentiated to rescue *FANCA*-deficient HPC progenitor function by repressing p53.[49] We found that in p53-repaired K562 cells, GAS6 could decrease p53 protein levels (Figure 7F). Therefore, we treated *FANCA*-deficient HPCs with or without recombinant human GAS6, finding that GAS6 treatment rescued HPC clonogenesis (Figure 7G). GAS6 did not diminish DNA damage as marked by formation of γH2AX (Figure 7H). Treatment of primary FA patient hematopoietic stem and progenitor cells could improve clonogenesis in all 4 patients tested in at least 1 of the GAS6 treatment durations (Figure 7I). These results identify GAS6 is a p53 target that can be modulated to improve FA HPC function.

Discussion

In this study, we used an inducible system to complement *FANCA* mutations in patient-derived IPSCs to maintain the function of the FA pathway while cells are in the pluripotent state.[22] By either removing or maintaining doxycycline exposure on initiation of EHT, we generated abundant fully complemented or uncomplemented human FA HPCs. These HPCs recapitulated key hallmarks of FA.[28,35,37] We identified GAS6 as a novel target of hyperactive p53 activity in FA HPCs and demonstrated that modulation of GAS6 signaling improves the function of *FANCA*-deficient HPCs.

Our system overcomes challenges faced over the past decade in the development of an IPSC-based human model of FA. Previous systems of hematopoietic differentiation have used either modified reprogramming methods or constitutive complementation of FA patient cells to generate IPSCs.[18-20,50] Alternatively, RNA interference has been used in non-FA pluripotent stem cells to disrupt the FA pathway.[51] Reprogramming under hypoxic conditions and with the addition of further transcription factors over the minimum required factors has been reported to enhance the efficiency of IPSC derivation from FA patient fibroblasts, although IPSCs from only 2 of 6 patient-derived fibroblast cultures could be propagated in this study.[20] Using this approach, post-reprogramming complementation was used to generate independent parallel control cell lines for use in functional analysis.[20] Although these approaches yield IPSCs that can undergo hematopoietic differentiation,[18] these cells maintain complementation constitutively, and so hematopoietic phenotypes caused by deficiency of the FA pathway are not evaluable and mechanisms of HPC dysfunction cannot be pursued. Alternatively, in rare uncomplemented FA patient-derived IPSC lines, the FA pathway can be repaired after reprogramming in order to generate isogenic, FA-expressing cells.[52] However, using our approach, one can readily derive isogenic FA-deficient and FA-competent hematopoietic cells from a single IPSC source. This system modulates *FANCA* expression at the time of hematopoietic specification and HPC emergence, mitigating confounding effects of *FANCA* deficiency on cells in the pluripotent state or during early germ layer patterning in EBs. Perhaps most importantly, this approach avoids comparison of IPSC lines derived from FA patients to those from healthy donors, where background genetic variability is well known to affect comparison of differentiation capacity.[24,53]

Our IPSC-derived, *FANCA*-deficient HPCs recapitulate key aspects of hallmark FA hematopoietic phenotypes. We found a highly reproducible defect in hematopoietic colony formation in HPCs derived from EBs and the StemDiff 2-dimensional differentiation system, as has been reported with primary patient FA cells.[28] Moreover, we find that *FANCA*-deficient, IPSC-derived HPCs show impaired cell cycle progression as has been demonstrated in both mouse models of FA and primary human cells,[54-56] as well as an impaired response to genotoxic stress.[57] Although the classic cell cycle defect in FA cells is a G2/M arrest, our findings of slowed G_1/S progression are consistent with prior observations of cell cycle defects in FA HPCs.[54,58] These results indicate that FA pathway deficiency may exert context-dependent effects on the cell cycle, in this case enhancing the G_1/S arrest that occurs during the transition from cycling multipotent/oligopotent progenitor to committed erythroid or myeloid progenitor.[44]

We used RNA sequencing to delineate the transcriptional divergence of otherwise isogenic *FANCA*-deficient and *FANCA*-expressing HPCs. Consistent with the phenotype of impaired clonogenicity, we found that *FANCA*-expressing HPCs maintained a signature of normal blood stem and progenitor cells relative to *FANCA*-deficient HPCs. Furthermore, distinct signatures related to cell cycle progression and DNA repair reflected known biology of the FA pathway.[54] Using unbiased GSEA against the Molecular Signatures Database,[30] we observed that *FANCA*-deficient HPCs showed a signature of erythroid differentiation relative to *FANCA*-expressing HPCs, leading us to validate this finding in functional studies. *FANCA*-deficient HPCs showed accelerated erythroid differentiation compared with FA-competent HPCs, a phenotype not previously described in FA. However, mice with germline FA pathway defects show depletion of phenotypic HPC populations with growth arrest that could represent rapid differentiation toward committed downstream lineages.[4,56] The combination of impaired colony-forming capacity and accelerated differentiation in *FANCA*-deficient HPCs supports a model wherein these cells rapidly lose HPC identity and more readily acquire a lineage-committed state. These findings illustrate the advantage of this system in providing a renewable source of human FA HPCs and isogenic control cells, as such primary patient derived HPCs are difficult to reproducibly investigate disease mechanisms.

Figure 7. (continued) ELISA experiments). (D) *FANCA*-expressing HPCs were treated with or without nutlin-3a and expression of *GAS6* measured by quantitative PCR (n = 3 biologic replicates results presented as mean ± SEM and compared by a Student *t* test with *P* value shown). (E) The indicated cells were treated either with BMS-777607 or GAS6 during EHT and then used in a colony formation assay (n = 7 biologic replicates over 3 experiments). (F) p53-repaired K562 cells were cultured serum free for 24 hours during which time they were treated with GAS6, and protein was collected for western blot analysis. (G) *FANCA*-deficient HPCs generated in the absence of doxycycline either in the presence of absence of recombinant GAS6 were harvested at day 5 of EHT and plated in methylcellulose medium, where colony formation was quantified after 14 days (n = 9 biologic replicates including 3 cell lines over 5 independent experiments). (H) Day 8 EHT cells generated without doxycycline and with or without GAS6 were exposed to mitomycin C and γH2AX-positive foci per cell quantified (n = 3 cell lines included and pooled in the overall analysis). (I) Primary FA patient bone marrow mononuclear cells were treated with or without GAS6 for either 3 or 7 days and then used in a colony formation assay, where colonies were quantified at day 14. All results presented as mean ± SEM and compared by a Student *t* test with *P* value shown.

FANCA-deficient HPCs show a delayed G_1/S phase transition with a diminished proportion of cells in S-phase compared with controls, recapitulating such findings observed in primary human FA CD34+ HPCs.[58] As reported previously, we find that this effect is associated with elevated activity of the p53-p21 axis, consistent with recapitulation of human FA disease phenotypes.[58] Intact MDM2-mediated p53 inhibition preserved HPC clonogenicity in *FANCA*-expressing cells, consistent with prior reports demonstrating that p53 activation in FA pathway deficiency impairs the growth and survival of HPCs.[59,60] In contrast, activation of p53 by pharmacologically impairing its interaction with MDM2 led to the loss of clonogenicity and acceleration of erythroid differentiation in *FANCA*-expressing HPCs. Conversely, disruption of the *TP53* gene in *FANCA*-deficient cells rescues clonogenicity and abates terminal differentiation. Given the known requirement of p21 activation for early erythroid commitment,[45] we suggest that the attenuated G_1/S transition induced by *FANCA* deficiency predisposes these cells to differentiation. Modulation of p53/p21 activity downstream of FA pathway mutations as a therapeutic approach should be considered with caution, given the accelerated tumorigenesis of p53-null mice bearing FA pathway mutations.[61] However, our results concur with the broader paradigm that cell cycle progression regulates differentiation propensity of stem and progenitor cells in a variety of tissues.[62,63]

We aimed to leverage our model of human FA to identify novel mechanisms of HPC dysregulation that could be targeted therapeutically. We found that hyperactive p53 in *FANCA*-deficient HPCs induced activation of GAS6, likely by directly binding the *GAS6* locus. Since GAS6 acts as a prosurvival, prohematopoietic factor,[48,49] we treated *FANCA*-deficient HPCs with recombinant GAS6, finding that this intervention was sufficient to partially rescue clonogenesis. These results are consistent with leveraging an endogenous negative feedback mechanism wherein potentiation of p53-induced GAS6 signaling may provide an intervention to improve hematopoiesis in FA, although this would in theory have to be accomplished in a selective manner given GAS6's reported protumorigenic effects.[64]

Compared with other diseases modeled with patient-derived IPSCs, FA has proven challenging because of the requirement for an intact FA DNA repair pathway for efficient reprogramming of somatic cells to pluripotency.[65] We used a doxycycline inducible system for inducible, reversible complementation of *FANCA*-deficient patient derived human IPSCs. This approach allowed us to generate isogenic *FANCA*-deficient and *FANCA*-expressing human HPCs that recapitulated key aspects of FA pathobiology, providing an indefinitely renewable source of human FA and otherwise isogenic control HPCs not obtainable in prior human IPSC-based models of FA. We used this system to discover a novel phenotype wherein FANCA-deficient, IPSC-derived HPCs undergo accelerated erythroid differentiation via a mechanism involving cell cycle regulation by p53 and p21. Our model provides a foundation for future studies of IPSC-based cellular therapy that could benefit patients with FA.

Acknowledgments

This study was supported by National Institutes of Health, National Institute of Diabetes, Digestive, and Kidney Diseases grants 1 K08 DK114527-01 (R.G.R.) and U54DK110805-02 (G.Q.D. and T.M.S.), and the Fanconi Anemia Research Fund (R.G.R. and G.Q.D.). S.I.W. was supported by National Institutes of Health, National Cancer Institute grant R01 CA102357 and a grant from the Fanconi Anemia Research Fund. E.L.d.R. was supported by a fellowship from the Coordination for the Improvement of Higher Education, Brazil.

Authorship

Contribution: W.M., S.B., S.R.-T., V.M., V.L., S.C., A.M.Z., O.A., C.K., Y.Z., T.M.S., and R.G.R. performed experiments; B.L.E., A.S., S.R.-T. and S.I.W. provided key reagents. S.B., S.R.-T., S.I.W., E.L.d.R., T.M.S., and R.G.R. analyzed data; and T.E.N., G.Q.D., S.I.W., and R.G.R. designed the research and wrote the manuscript.

Conflict-of-interest disclosure: During the conduct of this study, G.Q.D. held equity or received consulting fees from the following: Epizyme, 28/7 Therapeutics, and MPM Capital, LLC. The remaining authors declare no competing financial interests.

The current affiliation for E.L.d.R. is Department of Microbiology, Immunology, and Parasitology, Federal University of Santa Catarina, Florianopolis, Brazil.

The current affiliation for V.L. is Center for Hematology and Regenerative Medicine, Karolinska Institutet, Department of Medicine, Karolinska University Hospital, Huddinge, Stockholm, Sweden.

ORCID profiles: W.M., 0000-0003-3126-8432; S.B., 0000-0001-9937-0957; C.K., 0000-0002-7783-6602; O.A., 0000-0002-4961-077X; A.S., 0000-0002-4683-9958; T.M.S., 0000-0002-1599-9908; B.L.E., 0000-0003-0197-5451; R.G.R., 0000-0003-3620-2950.

Correspondence: R. Grant Rowe, Karp Family Research Building, 7th Floor, 1 Blackfan Cir, Boston, MA 02115; e-mail: grant_rowe@dfci.harvard.edu.

References

1. Kutler DI, Singh B, Satagopan J, et al. A 20-year perspective on the International Fanconi Anemia Registry (IFAR). *Blood*. 2003;101(4):1249-1256.
2. Zhang H, Kozono DE, O'Connor KW, et al. TGF-β inhibition rescues hematopoietic stem cell defects and bone marrow failure in fanconi anemia. *Cell Stem Cell*. 2016;18(5):668-681.
3. Zhang QS, Tang W, Deater M, et al. Metformin improves defective hematopoiesis and delays tumor formation in Fanconi anemia mice. *Blood*. 2016; 128(24):2774-2784.
4. Zhang QS, Marquez-Loza L, Eaton L, et al. Fancd2-/- mice have hematopoietic defects that can be partially corrected by resveratrol. *Blood*. 2010; 116(24):5140-5148.
5. Mehta PA, Tolar J. Fanconi anemia. Gene Reviews. 8 March 2018. https://www.ncbi.nlm.nih.gov/books/NBK1401/. Accessed 3 February 2020.
6. Pulliam-Leath AC, Ciccone SL, Nalepa G, et al. Genetic disruption of both Fancc and Fancg in mice recapitulates the hematopoietic manifestations of Fanconi anemia. *Blood*. 2010;116(16):2915-2920.

7. Carreau M, Gan OI, Liu L, et al. Bone marrow failure in the Fanconi anemia group C mouse model after DNA damage. *Blood*. 1998;91(8):2737-2744.
8. Cheng NC, van de Vrugt HJ, van der Valk MA, et al. Mice with a targeted disruption of the Fanconi anemia homolog Fanca. *Hum Mol Genet*. 2000;9(12):1805-1811.
9. Walter D, Lier A, Geiselhart A, et al. Exit from dormancy provokes DNA-damage-induced attrition in haematopoietic stem cells. *Nature*. 2015;520(7548):549-552.
10. Rowe RG, Daley GQ. Induced pluripotent stem cells in disease modelling and drug discovery. *Nat Rev Genet*. 2019;20(7):377-388.
11. Park IH, Arora N, Huo H, et al. Disease-specific induced pluripotent stem cells. *Cell*. 2008;134(5):877-886.
12. Takahashi K, Yamanaka S. Induction of pluripotent stem cells from mouse embryonic and adult fibroblast cultures by defined factors. *Cell*. 2006;126(4):663-676.
13. Takahashi K, Tanabe K, Ohnuki M, et al. Induction of pluripotent stem cells from adult human fibroblasts by defined factors. *Cell*. 2007;131(5):861-872.
14. Chadwick K, Wang L, Li L, et al. Cytokines and BMP-4 promote hematopoietic differentiation of human embryonic stem cells. *Blood*. 2003;102(3):906-915.
15. Wiles MV, Keller G. Multiple hematopoietic lineages develop from embryonic stem (ES) cells in culture. *Development*. 1991;111(2):259-267.
16. Tulpule A, Kelley JM, Lensch MW, et al. Pluripotent stem cell models of Shwachman-Diamond syndrome reveal a common mechanism for pancreatic and hematopoietic dysfunction. *Cell Stem Cell*. 2013;12(6):727-736.
17. Doulatov S, Vo LT, Macari ER, et al. Drug discovery for Diamond-Blackfan anemia using reprogrammed hematopoietic progenitors. *Sci Transl Med*. 2017;9(376):eaah5645.
18. Müller LU, Milsom MD, Harris CE, et al. Overcoming reprogramming resistance of Fanconi anemia cells. *Blood*. 2012;119(23):5449-5457.
19. Raya A, Rodríguez-Pizà I, Guenechea G, et al. Disease-corrected haematopoietic progenitors from Fanconi anaemia induced pluripotent stem cells. *Nature*. 2009;460(7251):53-59.
20. Suzuki NM, Niwa A, Yabe M, et al. Pluripotent cell models of Fanconi anemia identify the early pathological defect in human hemoangiogenic progenitors. *Stem Cells Transl Med*. 2015;4(4):333-338.
21. Yung SK, Tilgner K, Ledran MH, et al. Brief report: human pluripotent stem cell models of fanconi anemia deficiency reveal an important role for Fanconi anemia proteins in cellular reprogramming and survival of hematopoietic progenitors. *Stem Cells*. 2013;31(5):1022-1029.
22. Chlon TM, Ruiz-Torres S, Maag L, et al. Overcoming pluripotent stem cell dependence on the repair of endogenous DNA damage. *Stem Cell Rep*. 2016;6(1):44-54.
23. Sturgeon CM, Ditadi A, Awong G, Kennedy M, Keller G. Wnt signaling controls the specification of definitive and primitive hematopoiesis from human pluripotent stem cells. *Nat Biotechnol*. 2014;32(6):554-561.
24. Kilpinen H, Goncalves A, Leha A, et al. Common genetic variation drives molecular heterogeneity in human iPSCs [published correction in *Nature*. 2017;546:686]. *Nature*. 2017;546(7658):370-375.
25. Kajiwara M, Aoi T, Okita K, et al. Donor-dependent variations in hepatic differentiation from human-induced pluripotent stem cells [published correction in *Proc Natl Acad Sci USA*. 2012;109(36):14716]. *Proc Natl Acad Sci USA*. 2012;109(31):12538-12543.
26. Kyttälä A, Moraghebi R, Valensisi C, et al. Genetic variability overrides the impact of parental cell type and determines iPSC differentiation potential. *Stem Cell Reports*. 2016;6(2):200-212.
27. Ditadi A, Sturgeon CM, Tober J, et al. Human definitive haemogenic endothelium and arterial vascular endothelium represent distinct lineages. *Nat Cell Biol*. 2015;17(5):580-591.
28. Daneshbod-Skibba G, Martin J, Shahidi NT. Myeloid and erythroid colony growth in non-anaemic patients with Fanconi's anaemia. *Br J Haematol*. 1980;44(1):33-38.
29. Cahan P, Li H, Morris SA, Lummertz da Rocha E, Daley GQ, Collins JJ. CellNet: network biology applied to stem cell engineering. *Cell*. 2014;158(4):903-915.
30. Subramanian A, Tamayo P, Mootha VK, et al. Gene set enrichment analysis: a knowledge-based approach for interpreting genome-wide expression profiles. *Proc Natl Acad Sci USA*. 2005;102(43):15545-15550.
31. Kumari U, Ya Jun W, Huat Bay B, Lyakhovich A. Evidence of mitochondrial dysfunction and impaired ROS detoxifying machinery in Fanconi anemia cells. *Oncogene*. 2014;33(2):165-172.
32. Sumpter R Jr., Sirasanagandla S, Fernández AF, et al. Fanconi anemia proteins function in mitophagy and immunity. *Cell*. 2016;165(4):867-881.
33. Jaatinen T, Hemmoranta H, Hautaniemi S, et al. Global gene expression profile of human cord blood-derived CD133+ cells. *Stem Cells*. 2006;24(3):631-641.
34. Du W, Rani R, Sipple J, et al. The FA pathway counteracts oxidative stress through selective protection of antioxidant defense gene promoters. *Blood*. 2012;119(18):4142-4151.
35. Parshad R, Sanford KK, Jones GM. Chromosomal radiosensitivity during the G2 cell-cycle period of skin fibroblasts from individuals with familial cancer. *Proc Natl Acad Sci USA*. 1985;82(16):5400-5403.
36. Garbati MR, Hays LE, Keeble W, Yates JE, Rathbun RK, Bagby GC. FANCA and FANCC modulate TLR and p38 MAPK-dependent expression of IL-1β in macrophages. *Blood*. 2013;122(18):3197-3205.
37. Vanderwerf SM, Svahn J, Olson S, et al. TLR8-dependent TNF-(alpha) overexpression in Fanconi anemia group C cells. *Blood*. 2009;114(26):5290-5298.

38. Labbé E, Lock L, Letamendia A, et al. Transcriptional cooperation between the transforming growth factor-beta and Wnt pathways in mammary and intestinal tumorigenesis. *Cancer Res*. 2007;67(1):75-84.

39. Zhang QS, Benedetti E, Deater M, et al. Oxymetholone therapy of fanconi anemia suppresses osteopontin transcription and induces hematopoietic stem cell cycling. *Stem Cell Reports*. 2015;4(1):90-102.

40. Gillinder KR, Tuckey H, Bell CC, et al. Direct targets of pSTAT5 signalling in erythropoiesis. *PLoS One*. 2017;12(7):e0180922.

41. Lee HY, Gao X, Barrasa MI, et al. PPAR-α and glucocorticoid receptor synergize to promote erythroid progenitor self-renewal. *Nature*. 2015;522(7557):474-477.

42. Hu J, Liu J, Xue F, et al. Isolation and functional characterization of human erythroblasts at distinct stages: implications for understanding of normal and disordered erythropoiesis in vivo. *Blood*. 2013;121(16):3246-3253.

43. Choe KS, Radparvar F, Matushansky I, Rekhtman N, Han X, Skoultchi AI. Reversal of tumorigenicity and the block to differentiation in erythroleukemia cells by GATA-1. *Cancer Res*. 2003;63(19):6363-6369.

44. Matushansky I, Radparvar F, Skoultchi AI. Reprogramming leukemic cells to terminal differentiation by inhibiting specific cyclin-dependent kinases in G1. *Proc Natl Acad Sci USA*. 2000;97(26):14317-14322.

45. Papetti M, Wontakal SN, Stopka T, Skoultchi AI. GATA-1 directly regulates p21 gene expression during erythroid differentiation. *Cell Cycle*. 2010;9(10):1972-1980.

46. Boettcher S, Miller PG, Sharma R, et al. A dominant-negative effect drives selection of *TP53* missense mutations in myeloid malignancies. *Science*. 2019;365(6453):599-604.

47. Hietakangas V, Poukkula M, Heiskanen KM, Karvinen JT, Sistonen L, Eriksson JE. Erythroid differentiation sensitizes K562 leukemia cells to TRAIL-induced apoptosis by downregulation of c-FLIP. *Mol Cell Biol*. 2003;23(4):1278-1291.

48. Angelillo-Scherrer A, Burnier L, Lambrechts D, et al. Role of Gas6 in erythropoiesis and anemia in mice. *J Clin Invest*. 2008;118(2):583-596.

49. Onken J, Torka R, Korsing S, et al. Inhibiting receptor tyrosine kinase AXL with small molecule inhibitor BMS-777607 reduces glioblastoma growth, migration, and invasion in vitro and in vivo. *Oncotarget*. 2016;7(9):9876-9889.

50. Müller LU, Schlaeger TM, DeVine AL, Williams DA. Induced pluripotent stem cells as a tool for gaining new insights into Fanconi anemia. *Cell Cycle*. 2012;11(16):2985-2990.

51. Tulpule A, Lensch MW, Miller JD, et al. Knockdown of Fanconi anemia genes in human embryonic stem cells reveals early developmental defects in the hematopoietic lineage. *Blood*. 2010;115(17):3453-3462.

52. Liu GH, Suzuki K, Li M, et al. Modelling Fanconi anemia pathogenesis and therapeutics using integration-free patient-derived iPSCs. *Nat Commun*. 2014;5(1):4330.

53. Pashos EE, Park Y, Wang X, et al. Large, diverse population cohorts of hiPSCs and derived hepatocyte-like cells reveal functional genetic variation at blood lipid-associated loci. *Cell Stem Cell*. 2017;20(4):558-570.

54. Berger R, Le Coniat M, Gendron MC. Fanconi anemia. Chromosome breakage and cell cycle studies. *Cancer Genet Cytogenet*. 1993;69(1):13-16.

55. Rio P, Segovia JC, Hanenberg H, et al. In vitro phenotypic correction of hematopoietic progenitors from Fanconi anemia group A knockout mice. *Blood*. 2002;100(6):2032-2039.

56. Parmar K, D'Andrea A, Niedernhofer LJ. Mouse models of Fanconi anemia. *Mutat Res*. 2009;668(1-2):133-140.

57. Yoon YM, Storm KJ, Kamimae-Lanning AN, Goloviznina NA, Kurre P. Endogenous DNA damage leads to p53-independent deficits in replicative fitness in fetal murine Fancd2$^{-/-}$ hematopoietic stem and progenitor cells. *Stem Cell Rep*. 2016;7(5):840-853.

58. Ceccaldi R, Parmar K, Mouly E, et al. Bone marrow failure in Fanconi anemia is triggered by an exacerbated p53/p21 DNA damage response that impairs hematopoietic stem and progenitor cells. *Cell Stem Cell*. 2012;11(1):36-49.

59. Li X, Wilson AF, Du W, Pang Q. Cell-cycle-specific function of p53 in Fanconi anemia hematopoietic stem and progenitor cell proliferation. *Stem Cell Rep*. 2018;10(2):339-346.

60. Hu L, Huang W, Bei L, Broglie L, Eklund EA. *TP53* haploinsufficiency rescues emergency granulopoiesis in *FANCC*$^{-/-}$ mice. *J Immunol*. 2018;200(6):2129-2139.

61. Freie B, Li X, Ciccone SL, et al. Fanconi anemia type C and p53 cooperate in apoptosis and tumorigenesis. *Blood*. 2003;102(12):4146-4152.

62. Pauklin S, Vallier L. The cell-cycle state of stem cells determines cell fate propensity [published correction in *Cell*. 2013;156(6):P1338]. *Cell*. 2013;155(1):135-147.

63. Ruijtenberg S, van den Heuvel S. G1/S inhibitors and the SWI/SNF complex control cell-cycle exit during muscle differentiation. *Cell*. 2015;162(2):300-313.

64. Gomes AM, Carron EC, Mills KL, et al. Stromal Gas6 promotes the progression of premalignant mammary cells. *Oncogene*. 2019;38(14):2437-2450.

65. Shi Y, Inoue H, Wu JC, Yamanaka S. Induced pluripotent stem cell technology: a decade of progress. *Nat Rev Drug Discov*. 2017;16(2):115-130.